ISSN: 2472-3703 DOI: 10.6911/WSRJ.202511_11(11).0003

Study on Elastohydrodynamic Lubrication Characteristics of Grease-Lubricated Spur Gears

Longhua Tang *, Zhibo Tang

School of Mechanical Engineering, Xihua University, Chengdu 610039, China

* Corresponding author: (Email: 2924275784@qq.com)

Abstract

To reveal the evolution mechanism of the lipid film at the meshing interface of involute spur gears, an elastohydrodynamic lubrication (EHL) numerical model for line contact of lipid-lubricated spur gears was established based on the Ostwald constitutive equation. The oil film pressure and thickness distributions along the meshing line were obtained by using a numerical iterative algorithm combined with the multi-grid technique. On this basis, the influence laws of key operating parameters (gear speed, transmitted torque and lipid viscosity) on the elastohydrodynamic lubrication characteristics were systematically investigated. The results show that under lipid lubrication conditions, when the gear speed increases, the entrainment velocity increases accordingly, which is more conducive to the formation of the lubricating oil film, resulting in an increase in the oil film thickness. When the transmitted torque increases, the oil film thickness will slightly decrease. In addition, when the lipid viscosity increases, the position of the secondary pressure peak in the gear contact area shifts towards the inlet area, significantly increasing the oil film thickness. However, it is not advisable to pursue excessively high lipid viscosity, as the macroscopic rheology of the lipid, gear churning loss and lipid supply state should also be comprehensively considered. Therefore, in practical applications, when selecting a lipid for gears, the specific working conditions must be fully considered to ensure the best lubrication performance.

Keywords

Spur gears; Grease; Elastohydrodynamic lubrication; Oil film characteristics.

1. INTRODUCTION

Gear transmission is one of the primary drive mechanisms in modern industrial machinery, playing a crucial role in aerospace, automotive, marine, mining, and other industries. Lubrication is a vital factor in fully utilizing gear load-bearing capacity, reducing the likelihood of gear failure, extending gear service life, and enhancing transmission efficiency. Currently, lubricating oils and greases are commonly used lubricants. As a semi-solid colloidal dispersion system, grease is widely applied across numerous fields due to its outstanding anti-friction and anti-wear properties [1]. Compared to oil lubrication, grease offers superior sealing performance and adhesion. It can adhere to vertical surfaces without leakage at room temperature, eliminating the need for complex internal oil passage or collection structures. Grease lubrication also enables equipment light weighting, allowing gearboxes to reduce mass without compromising reliability, thereby enhancing equipment survivability [2-3]. In low-speed, heavy-load, or micro-mechanical transmission scenarios, oil lubrication struggles to form sufficiently thick lubricating films, leading to wear. Test results confirm that under

ISSN: 2472-3703 DOI: 10.6911/WSRJ.202511_11(11).0003

boundary lubrication conditions, grease demonstrates superior anti-wear performance compared to traditional mineral oils [4-5].

Currently, in the field of elastohydrodynamic lubrication (EHL) for involute spur gears, research on oil-based EHL has reached a relatively mature stage. Based on the theory of line-contact EHL, Qiuju Wang et al. [6] focused on high-speed, heavy-load cylindrical gears in aircraft engines. Through numerical analysis, they investigated the influence patterns of varying power, rotational speeds, and temperatures on gear lubrication performance. Junjie He [7] examined a series of elastohydrodynamic lubrication issues, including smooth-surface-to-rough-surface contact, full-film-to-partial-film hybrid lubrication, and line-to-point contact, ultimately establishing a deterministic hybrid elastohydrodynamic lubrication model for involute gears. Han Wang[8] and colleagues investigated tooth surface wear in straight gears under hybrid elastohydrodynamic lubrication conditions. Lin Zhang [9] investigated the critical relationship between oil film stiffness excitation and system vibration response under various operating conditions based on line-contact elastohydrodynamic lubrication theory. Jia'ao Zhou et al. [10] conducted oil-lubricated elastohydrodynamic studies on steel-polymer spur gear pairs, revealing the effects of pressure angle, load, and rotational speed on oil film thickness.

However, research on the film formation mechanism, rheological processes, and film thickness of grease-lubricated spur gears remains insufficient. Therefore, understanding grease film formation in gears and predicting film thickness becomes particularly crucial.

2. GEAR GEOMETRIC MODEL

2.1. Solve for the Combined Radius of Curvature, Entrainment Velocity, And Slide–Rolling Ratio

To conduct the study on the lubrication and flow of grease for involute spur gears, it is necessary to calculate the geometric parameters, entrainment velocity, contact load and other key parameters at each point along the meshing line of the tooth profile. Two finite-length equivalent cylindrical rollers are used to simulate the transient sliding-rolling contact process of the gears. The gear meshing process is shown in Figure 1.

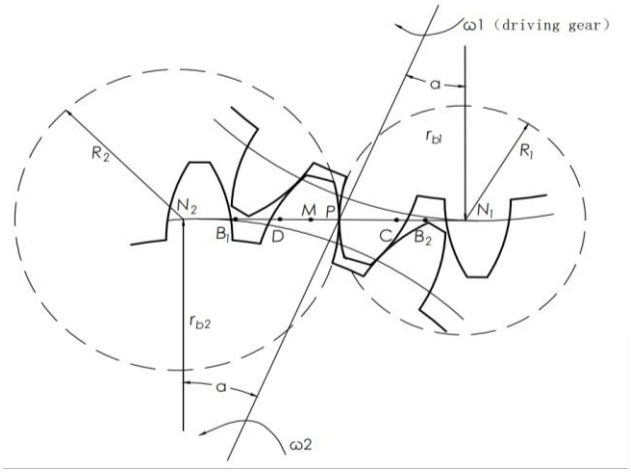

Figure 1. Schematic diagram of gear meshing

N_1N_2 represents the theoretical meshing line, B_2B_1 represents the actual meshing line, rb_1 and rb_2 are the base circle radii of the two gears, r_1 and r_2 are the pitch circle radii of the two gears, and α is the pressure angle. P is the node, C is a point at the root of the driving gear, D is a point at the top of the driving gear, M is a meshing point on the tooth profile of the driving gear, the distance from M to the center of the driving gear is r_M, and the distance from point M to the

ISSN: 2472-3703 DOI: 10.6911/WSRJ.202511_11(11).0003

node P is L_{PM}. R_1 and R_2 are the radii of curvature of the two cylindrical rollers at the meshing point M, and i is the gear transmission ratio.

$$L_{PM} = \pm\sqrt{(r_1 \sin\alpha)^2 - (r_1)^2 + r_M^2} \mp r_1 \sin\alpha \tag{1}$$

$$R_1 = r_1 \sin\alpha \pm L_{PM} \tag{2}$$

$$R_2 = r_2 \sin\alpha \mp L_{PM} \tag{3}$$

Thus, the combined radius of curvature at the meshing point is as follows:

$$\frac{1}{R} = \frac{1}{R_1} + \frac{1}{R_2} \tag{4}$$

The tangential velocities of the driving and driven gears at the point are as follows:

$$u_1 = \omega_1 \times R_1 \tag{5}$$

$$\mathrm{u}_2 = \omega_2 \times \mathrm{R}_2 \tag{6}$$

Tooth surface entrainment velocity and slide–rolling ratio are as follows:

$$u_s = \frac{u_1 + u_2}{2} \tag{7}$$

$$q = \frac{u_1 - u_2}{u_s} = \frac{2(R_1 + iR_2)}{R_1 - iR_2} \tag{8}$$

2.2. Tooth Surface Contact Load Analysis

For involute cylindrical gear drives, it is necessary to consider that the overlap is greater than 1, so there are single-tooth and double-tooth meshing zones, and consider the load distribution [11-12].

$$w = \frac{T_1}{mLr_M \cos\alpha} \tag{9}$$

Here, w represents the load per unit length of the tooth width, m represents the number of pairs involved in meshing, and L represents the contact length.

Tooth surface contact stress can be expressed as:

$$\sigma_{eq} = \left(\frac{E' F_n}{2\pi R}\right)^{0.5} \tag{10}$$

The equivalent elastic modulus is usually expressed and is usually defined as:

$$\frac{1}{E'} = \frac{1-\nu_1^2}{E_1} + \frac{1-\nu_2^2}{E_2} \tag{11}$$

ISSN: 2472-3703 DOI: 10.6911/WSRJ.202511_11(11).0003

E_1, E_2 and v_1, v_2 respectively represent the Young's modulus and Poisson's ratio of the tooth surfaces of the driving wheel and the driven wheel.

3. ELASTOHYDRODYNAMIC LUBRICATION MODEL

3.1. Reynolds Equation

Assuming that the grease supply is sufficient during gear operation, study the characteristics of the grease in a non-starvation state. The grease is composed of base oil and thickener, and its viscosity changes at different pressures. When the shear force generated by the relative sliding of the tooth surface exceeds the ultimate shear stress of the grease, the grease behaves as a non-Newtonian fluid under this condition.

The following three accurate constitutive equations can describe the rheological behavior of lubricating grease [13]:

$$\tau = \eta\dot{\gamma}^n (Ostwald) \tag{12}$$

$$\tau = \tau_s + \eta\dot{\gamma} (Bingham) \tag{13}$$

$$\tau = \tau_s + \eta\dot{\gamma}^n (Herschel - Bulkley) \tag{14}$$

In the elastohydrodynamic studies, grease is widely using the Ostwald rheological model. In this paper, based on the Ostwald constitutive model, a one-dimensional Reynolds equation for grease lubrication is established as follows:

$$\frac{n}{2n+1} \cdot \left(\frac{1}{2}\right)^{\frac{n+1}{n}} \left\{ \frac{d}{dx} \left[\rho h^{\frac{2n+1}{n}} \left(\frac{1}{\eta} \frac{dp}{dx} \right)^{\frac{1}{n}} \right] \right\} = u_s \frac{d(\rho h)}{dx} \tag{15}$$

Boundary conditions of the Reynolds equation:

$$\begin{cases} p|(x = x_{in}) = 0 \\ p|(x = x_{out}) = 0 \\ p|(x_{in} < x < x_{out}) > 0 \end{cases} \tag{16}$$

x_{in}, x_{out} respectively represent the coordinates of the lubricating oil film inlet and outlet within the calculation area.

3.2. Film Thickness Equation

$$h(x) = h_0 + \frac{x^2}{2R} - \frac{2}{\pi E'} \int_{x_{in}}^{x_{out}} p\,(s)\, ln(\,x - s)^2 ds \tag{17}$$

3.3. Viscosity–pressure Equation and Density–Pressure Equation

Density–pressure equation [14]

$$\rho = \rho_0 \left(1 + \frac{0.6p}{1+1.7p}\right) \tag{18}$$

Viscosity–pressure equation [15]

$$\eta = \eta_0\, exp((ln\eta_0 + 9.67) \times (-1 + (1 + p/p_0)^Z)) \tag{19}$$

ISSN: 2472-3703 DOI: 10.6911/WSRJ.202511_11(11).0003

3.4. Load Equation

$$w - \int_{x_{in}}^{x_{out}} p\,(x)dx = 0 \tag{20}$$

4. RESULT AND DISCUSSION

4.1. Analysis of the Elastic Flow Characteristics of Gear Grease Lubrication

Parameters of involute straight gear transmission: The number of teeth of the driving and driven wheels are $z_1 = 21$ and $z_2 = 35$ respectively, the pressure angle is 20°, the gear module is m = 2mm, the tooth width is 20mm, the overlap degree is 1.617, the gear material is 40Cr, the elastic modulus and Poisson's ratio are $E_1 = E_2 = 2.06\text{x}10^{11}$ Pa and $v_1 = v_2 = 0.3$ respectively. The torque of the driving wheel is 24 N·m, the rotational speed of the driving wheel is 500 r/min, the viscosity of the lubricating grease $\eta_0 = 0.4$ Pa·s, and the flow rate index n = 0.85.

The curvature radius and entrainment velocity along the meshing line vary as shown in Figures 2 and 3. The combined curvature radius R at the meshing point first increases to near the node and then decreases. The speed at the meshing point on the driving wheel gradually increases, the speed at the meshing point on the driven wheel gradually decreases, and the suction speed gradually increases. The slide–rolling ratio and contact load are shown in Figures 4 and 5, where the slide–rolling ratio is negative from the root circle to the pitch circle, positive from the pitch circle to the tip circle, and 0 at the pitch circle. As can be seen from Figure 5, the contact load changes significantly from the single-tooth meshing zone to the double-tooth meshing zone, with the load in the single-tooth meshing zone being almost twice that in the double-tooth meshing zone.

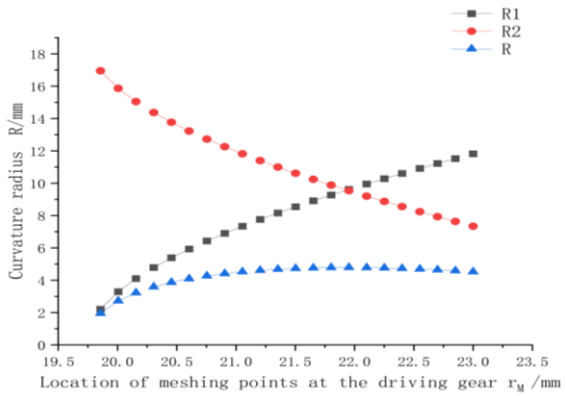

Figure 2. Curvature radius changes along the meshing line

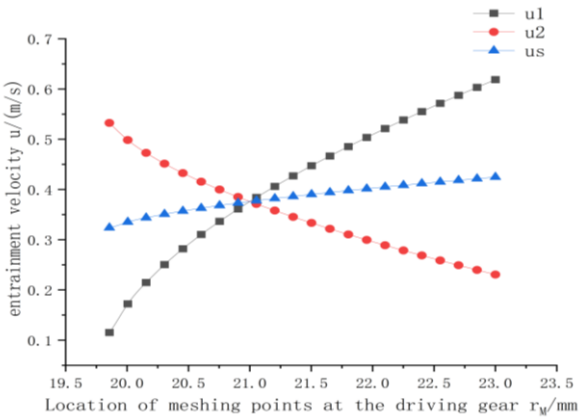

Figure 3. Diagram of the entrainment velocity along the meshing line

ISSN: 2472-3703 DOI: 10.6911/WSRJ.202511_11(11).0003

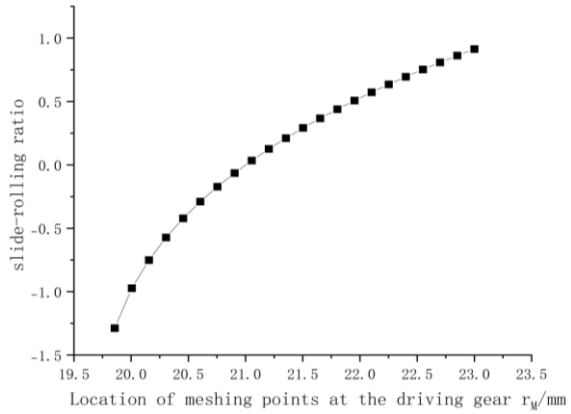

Figure 4. Variation of the slide–rolling ratio along the meshing line

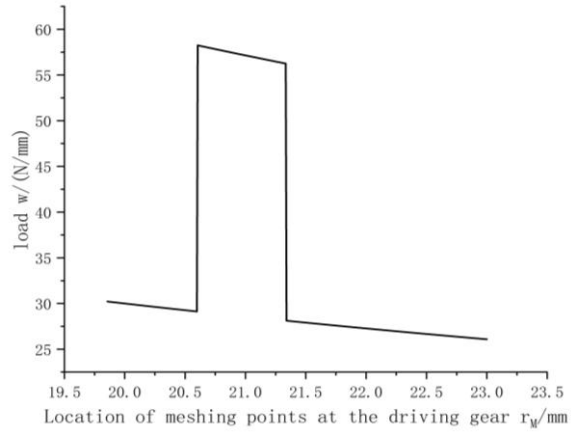

Figure 5. Load changes along the meshing line

Under the condition of sufficient lubricant supply during the gear meshing process, in order to study the lubrication characteristics of the grease at different positions on the tooth profile, the calculated data of the tooth root position C, the node position P, and the tooth tip position D on the driving gear were selected for analysis. The results are shown in Figure 6. Due to the high-frequency dynamic changes of the entrainment speed and load at the meshing point of the gears, the central compressive stress and the central grease film thickness also change dynamically during each tooth surface meshing process. Because in the oil film outlet area, the oil film pressure returns to the ambient pressure, resulting in oil film rupture, hindering the flow of the lubricating grease, causing the grease to accumulate, and forming a local secondary pressure peak. At the secondary pressure peak, due to the contraction of the grease film, the necking phenomenon occurs in the outlet area. When just entering the meshing, the entrainment speed at point C is lower than at other points, and the pressure at the peak position reaches 0.801GPa, with the central film thickness being 0.122 um, and the minimum film thickness at the necking point is 0.091 um. At the node P position, since it is in the single-tooth meshing area, the load is twice that of point C, but the comprehensive curvature radius and entrainment velocity have improved, with the central film thickness being 0.135 um, and the minimum film thickness being 0.099 um. The pressure at point D is smaller than at other points, and the entrainment speed is the highest. The central film thickness is 0.152 um, and the minimum film thickness is 0.114 um, which has increased significantly compared to other points.

ISSN: 2472-3703 DOI: 10.6911/WSRJ.202511_11(11).0003

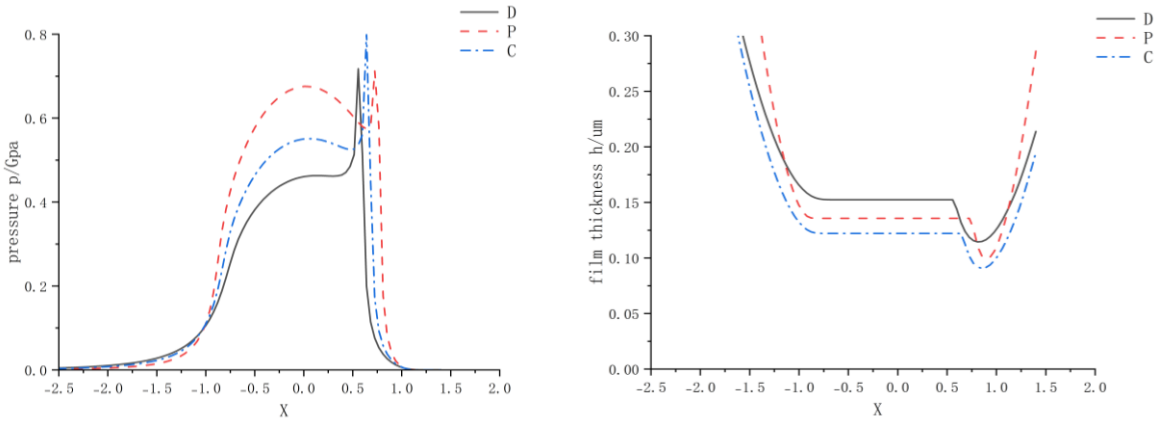

(a) Oil film pressure variation curve (b) Oil film thickness distribution curve

Figure 6. 0il film pressure and oil film thickness at characteristic points on meshing line

4.2. Effects of Different Operating Conditions on The Elastohydrodynamic Characteristics of Gear Grease Lubrication

During the actual use of gears, the operating parameters of the gear system vary greatly. Therefore, it is necessary to investigate the influence of different gear speeds, torques and grease viscosity on the elastohydrodynamic characteristics of gear grease lubrication.

4.2.1. The effect of rotational speed on the elastohydrodynamic properties of gear grease lubrication

When the driving wheel torque is 24 N·m, the driving wheel speeds are 250,500 and 750 r/min. With grease viscosity η_0= 0.4 Pa·s and rheological index n = 0.85, observe the changes in oil film pressure and film thickness at node P. Figure 7 shows the lubricating grease oil film pressure and oil film thickness variations at the node position under different gear speeds. As the gear speed increases, the entrainment velocity at the node position also increases, leading to a corresponding increase in film thickness. Simultaneously, the height of the secondary pressure peak rises with increasing speed. When the speed reaches 750 r/min, the secondary peak pressure exceeds the central film thickness pressure.

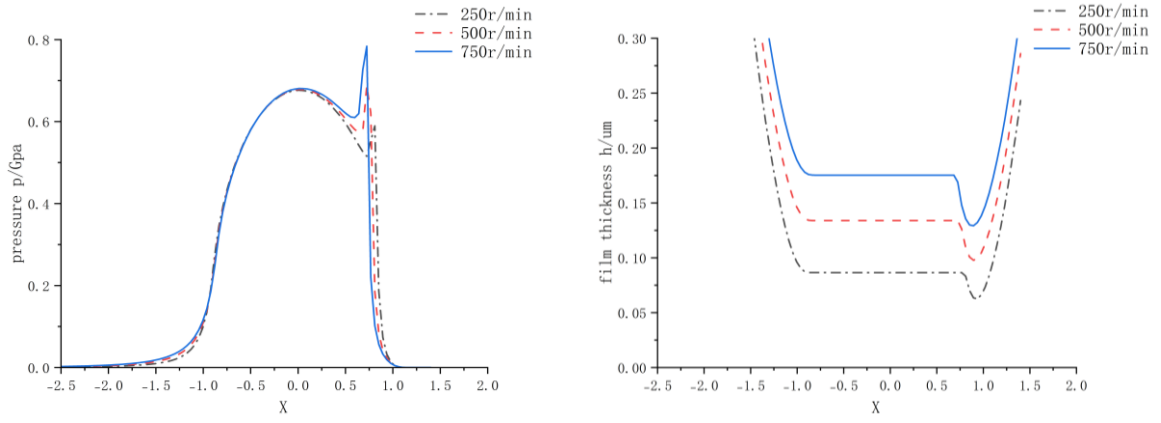

(a) Oil film pressure variation curve (b) Oil film thickness distribution curve

Figure 7. Oil film pressure and oil film thickness at different rotational speeds

4.2.2. The effect of torque on the elastohydrodynamic characteristics of gear grease lubrication

When the driving wheel speed is 500 r/min, the driving wheel torque is 12,24 and 36 N·m. With grease viscosity η_0= 0.4 Pa·s, calculate the oil film pressure and film thickness at the gear

ISSN: 2472-3703 DOI: 10.6911/WSRJ.202511_11(11).0003

node position. Figure 8 indicates that as the load increases, the secondary pressure peak shifts toward the outlet position, with the necking phenomenon becoming more pronounced. Both the center film thickness and minimum film thickness show a decreasing trend, though the magnitude of change is relatively small.

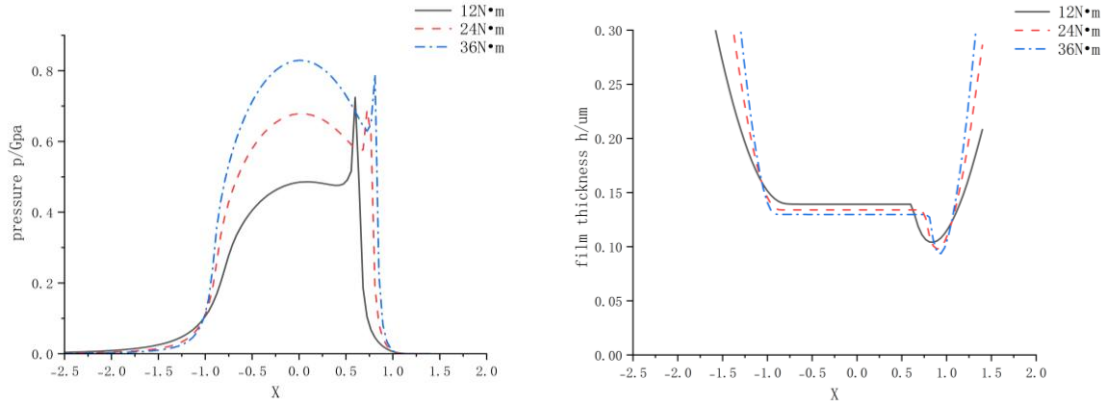

(a) Oil film pressure variation curve (b) Oil film thickness distribution curve

Figure 8. Oil film pressure and oil film thickness at different torques

4.2.3. The effect of viscosity on the elastohydrodynamic properties of gear grease lubrication

When the drive wheel torque is 24 N·m and the drive wheel speed is 500 r/min, observe the changes in oil film pressure and film thickness at node P under lubricating grease with viscosity η_0= 0.1、0.4、0.8 Pa·s and rheological index n=0.85. As shown in Figure 9, with increasing grease viscosity, the secondary pressure peak gradually rises while shifting toward the inlet region. Concurrently, the film thickness significantly increases, with the minimum thickness rising from 0.031 um to 0.154 um.

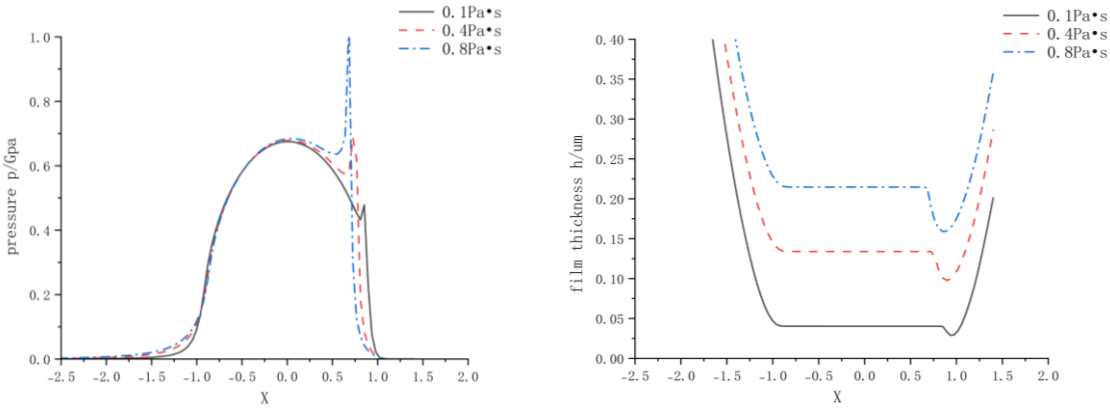

(a) Oil film pressure variation curve (b) Oil film thickness distribution curve

Figure 9. Oil film pressure and thickness of nodes at different viscosities

5. CONCLUSIONS

(1) Since the entrainment velocity and the combined radius of curvature on the meshing line increase gradually from the meshing point to the meshing point, and there is relative sliding on the tooth surface. Therefore, for one meshing cycle, the gear lubrication process is actually discontinuous, and a new oil film needs to be established with each meshing.

(2) The entrainment speed at the tooth root position is the lowest, the load is the largest, and the oil film thickness is the thinnest at the tooth root position. The oil film thickness at the tooth tip position is larger, and the thickness of the node oil film is in the middle.

ISSN: 2472-3703 DOI: 10.6911/WSRJ.202511_11(11).0003

(3)As the rotational speed increases, the entrainment speed also increases, which helps to form a better grease film and increase the thickness of the oil film; as the torque increases, the film thickness decreases (with a relatively small impact); as the viscosity increases, the secondary pressure peak moves towards the inlet area, and the oil film thickness significantly increases. However, in practical applications, in addition to the high viscosity characteristic of the grease, the macroscopic rheology of the grease in the gearbox and the efficiency issue caused by the oil mixing loss should also be considered.

REFERENCES

[1] Chen, J. (2010). Synthesis, characterization, and tribological behavior of neopentyl polyol ester-based and mixed oil-based titanium complex grease. Tribology Letters, 40(1), 149-154.

[2] Yinbin Zhou, Wenbin Pan, Chuan Liu, et al. Discussion on Key Technologies of Helicopter Grease-Lubricated Reducer [J]. Aeronautical Power, (in Chinese) 2023, (01):43-45.

[3] Lugt, Piet M. "A review on grease lubrication in rolling bearings." Tribology Transactions52.4 (2009): 470-480.

[4] Schultheiss H, Tobie T, Michaelis K, et al. The slow-speed wear behavior of case-carburized gears lubricated with NLGI 00 grease under boundary lubrication conditions. Tribology Transactions, 2014, 57(3): 524-532.

[5] Li X, Guo F, Poll G, et al. Grease film evolution in rolling elastohydrodynamic lubrication contacts. Friction, 2021, 9: 179-190.

[6] Qiuju Wang, Zhengang Liu, Hengwen Qiao, et al. Numerical Analysis of Elastic Flow Lubrication for High-Speed and Heavy-Duty Cylindrical Gears [J]. Lubrication and Sealing, (in Chinese) 2022, 47(03):102-109.

[7] Junjie He. Analysis of Mixed Lubrication for Involute Gears Based on Deterministic Model [D]. Nanjing University of Aeronautics and Astronautics, (in Chinese) 2011.

[8] Han Wang, Huilan Li, Guofeng Liu, et al. Research on Tooth Surface Wear of Straight Bevel Gears under Mixed Turbulent Lubrication [J]. Mechanical Transmission, (in Chinese) 2022, 46(12):31-37. DOI:10.16578/j.issn.1004.2539.2022.12.005.

[9] Lin Zhang. Research on the Dynamic Characteristics of a Two-stage Straight Gear Transmission System Considering Gear Lubrication [D]. Xinjiang University, 2021. DOI:10.27429/d.cnki.gxjdu.2021.000183.

[10] Jiaohao Zhou, Xiaoling Liu, Qun Li, et al. Analysis of Elastic Flow Lubrication for Steel-Polymer Straight Gear Pair [J]. Mechanical Transmission (in Chinese) 2024, 48(07):114-120. DOI:10.16578/j.issn.1004.2539.2024.07.014.

[11] Johnson K L. Contact mechanics. Cambridge university press, 1987.

[12] Larsson R. Transient non-Newtonian elastohydrodynamic lubrication analysis of an involute spur gear. Wear, 1997, 207(1-2): 67-73.

[13] Shizhu Wen, Ping Huang. Principles of Tribology [M]. Tsinghua University Press. (in Chinese) 2012.

[14] Dowson D, Higginson G R. Elastohydrodynamic Lubrication: The Fundamentals of Roller and Geer Lubrication [M]. Pergamon Press, 1966.

[15] Roelands C J. Correlational Aspects of the Viscosity-Temperature-Pressure Relationship. Doctoral Thesis, Technological University of Deft, 1966.